Chapter 5

Coarse circuit switching in the core

5.1 Introduction

In Chapters 1, 2 and 3, we have seen how we can benefit from having more circuit switching in the core of the Internet; circuit switching allows us to build switches with fast all-optical data paths. Moreover, circuit switching can provide higher capacity and reliability than packet switching without degrading end-user response time. Chapter 4 described TCP Switching, an evolutionary way of integrating a circuit-switched backbone with the rest of the Internet. This integration of circuit and packet switching was done by mapping application flows to fine-grain, lightweight circuits.

One problem of TCP Switching is that currently most crossconnects in circuit switches cannot switch at the 56-Kbit/s granularity that was proposed in Chapter 4.[1] It would be extremely wasteful to reserve an STS-1 channel or a wavelength exclusively for a single user flow whose peak rate is limited to only 56 Kbit/s by its access link. Another shortcoming, caused by several crossconnect technologies and signaling mechanisms in circuit switching, is that it may take tens or hundreds of milliseconds to reconfigure the switch or to exchange the signaling messages that create a new circuit. These long circuit-creation latencies occur when the crossconnect has to

[1] Typically, electronic SONET circuit switches use circuit granularities of STS-1 (51 Mbit/s) or higher, whereas DWDM switches have granularities of OC-48 (2.5 Gbit/s) or higher.

move electromechanical parts, such as MEMS mirrors, or when the signaling requires a positive acknowledgement from the egress circuit switch.

This chapter addresses these two limitations of circuit-switching technologies. More precisely, it explores ways of using circuit switching in the Internet when cross-connects have granularities that are much larger than the peak rate of user flows, and when circuit switches are slow to reconfigure.

In this chapter, I propose monitoring the bandwidth that is carried by all user flows between each pair of boundary routers around a circuit-switched cloud in the core. This measurement provides an anticipating and stable estimation of the traffic matrix that is then used to properly size the coarse-granularity circuits that interconnects the boundary routers. In order to compensate for the circuit-creation latency of the network, I propose allocating these circuits using an additional safeguard band that prevents the circuits from overflowing.

One of the themes developed in Chapter 4 is again the basis for this chapter; namely, how one can configure the circuit-switched backbone by monitoring the activity of user flows. The difference is that now a core circuit is carrying many user flows simultaneously, and so the mapping between user flows and circuits is not as straightforward as that discussed in Chapter 4. It is no longer a matter of when to create the circuits but how much capacity to assign to them.

5.1.1 Organization of the chapter

Section 5.2 defines the problem addressed in this chapter and describes other approaches that have been proposed by other researchers. Section 5.3 shows how one can control a circuit-switched Internet core by monitoring user flows. Section 5.4 builds a model for the buildup of user flows. Then, Section 5.5 discusses some of the implications of this approach. Finally, Section 5.6 concludes this chapter.

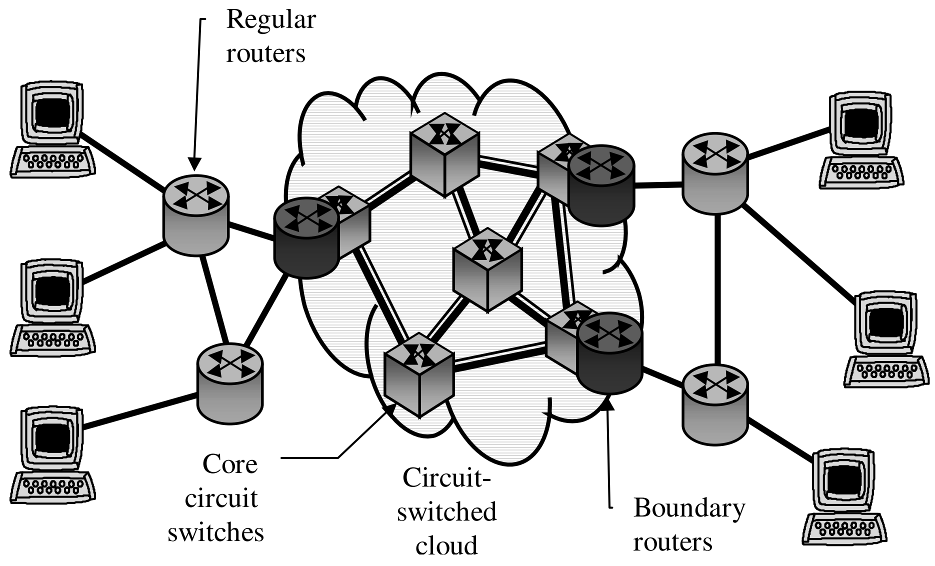

Figure 5.1: Network topology considered in this chapter.

5.2 Background and previous work

Consider the network architecture shown in Figure 5.1. The problem that arises now is how to accommodate traffic between boundary routers around the circuit-switched cloud. This issue can be decomposed in two parts: First, how much capacity is needed between boundary routers? (i.e., what is the traffic matrix between boundary routers?). Second, once we know this traffic matrix, how do we create the circuits that provide the required capacity?

The second question has been looked at by several researchers before. In some cases, it is regarded as a centralized optimization problem, in which the total throughput of the network needs to be maximized subject to constraints on link capacity and maximum flow rate. The problem is either solved using integer linear programming or some heuristic that achieves an approximate, but faster, solution [9, 163, 176]. The output of this centralized optimization problem is then distributed to the circuit switches. In other cases, researchers have treated the problem as an incremental problem in which each circuit request is routed individually as it arrives [169, 8, 13]. The circuit routing can be done at the source or hop-by-hop. Chapter 6 describes some of these signaling and routing protocols that have been proposed.

(a)

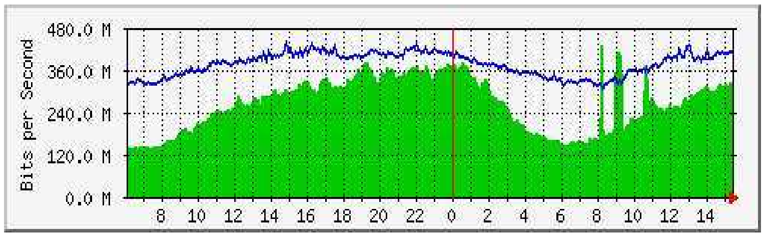

(b)

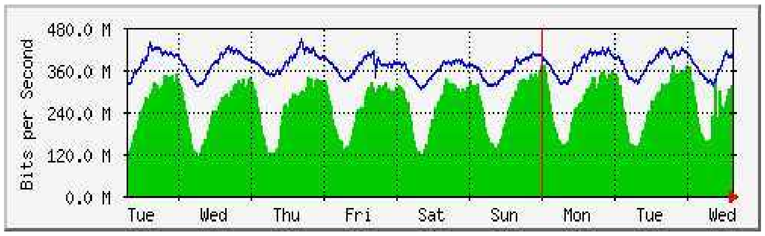

(c)

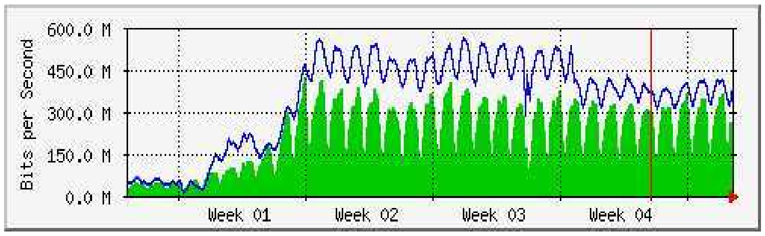

Figure 5.2: Daily (a), weekly (b) and monthly (c) average traffic traces in a 1-Gbit/s Ethernet link between Purdue University and the Indiana GigaPoP connecting to Internet-2 [63], as observed on February 5th, 2003. The dark line indicates outgoing traffic; the shaded area indicates incoming traffic. The low traffic in weeks 0 and 1 in graph (c) corresponds to the last week of December 2002 and the first week of January 2003, respectively, when the university was in recess.

This chapter focuses on the first question, how to estimate the traffic matrix between boundary routers and then use the estimate to provision coarse-granularity circuits. Some researchers [9, 163, 120] have suggested that future traffic matrices can be predicted off-line using past observations. These researchers point out that traffic in the core of the network is smoother than at the edges and that it follows strong hourly and daily patterns that are easy to characterize, as shown in Figure 5.2. For example, traffic is affected by human activity and scheduled tasks, and so peak traffic occurs during work hours on weekdays, whereas at night and during weekends there is less traffic.

Nonetheless, this off-line prediction of the traffic matrix fails to forecast sudden changes in traffic due to external events, such as breaking news that creates flash crowds, a fiber cut that diverts traffic or the new version of a popular program that generates many downloads. Only an on-line estimation of the traffic matrix would be able to accommodate these sudden and unpredictable changes in traffic patterns.

This on-line estimation of traffic could be done in several ways. One of them is to monitor the aggregate packet traffic [79], either by observing the instantaneous link bandwidth or the queue sizes in the routers. While this approach does not require much hardware support and is easy to implement, it does not provide good information about the traffic trends. Packet arrivals present many short- and long-range dependencies that make both the instantaneous arrival rates and queue sizes fluctuate wildly. In contrast, I propose using another way of estimating the current traffic usage by monitoring user flows. It requires more hardware support, but, in exchange, user flows provide a traffic estimation that is more predictive and has less variation, at least for the circuit-creation latencies under consideration (1 ms-1 s), as we will see below.

Figure 5.3 gives a clear example of the fluctuations in the instantaneous arrival rate. The dots in the background denote the instantaneous link bandwidth over 1-ms time intervals. With so much noise, it is difficult to see any trends in the data rates. Thus, one could apply filters to smooth the signal. For example, the dark gray line in Figure 5.3 shows the moving average $R(t) = (1 - \alpha)R(t - \Delta t) + \alpha r(t)$, where $r(t)$ is the instantaneous measure, Δt is 1 ms and α is 0.10. The figure also shows the instantaneous traffic rate over 100-ms intervals (light gray line) and the sum of the average bandwidth of the active flows (black line). The average bandwidth of a flow is the total number of bits that are transmitted divided by the flow duration. Of course, the flow average bandwidth is something that is not known when a flow starts, but I will explain below how to estimate an upper bound in the next section. One can see that the 100-ms bin size provides the signal with the least noise of all measures of traffic based on counting packets, but there are still many more fluctuations than in the measure based on the average bandwidth of active flows, from which the trends are much clearer. In brief, user flows provide more stable measurement than packets and queue sizes for time scales between 1 ms and 1 s.

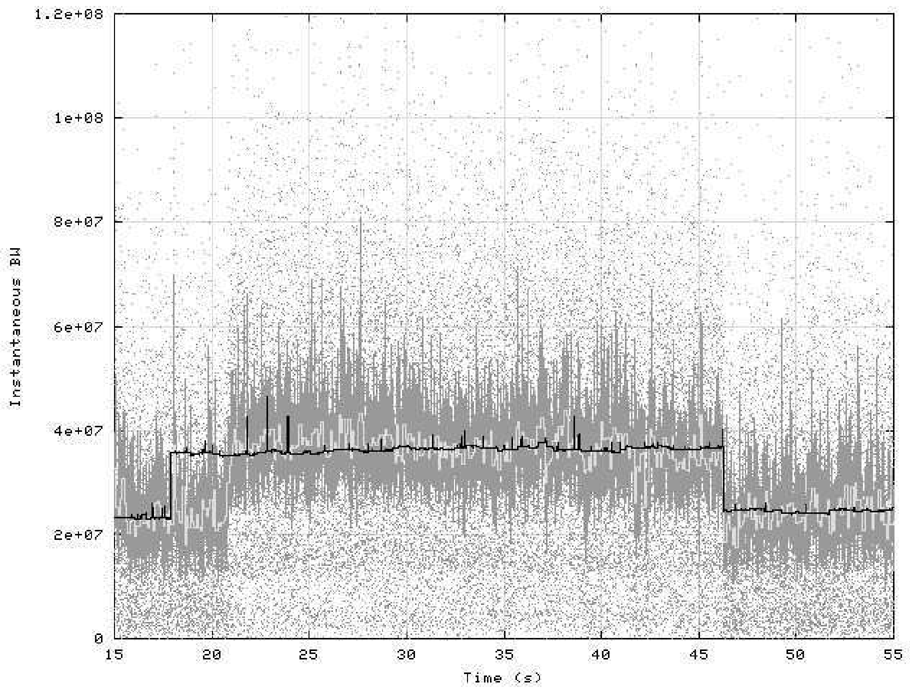

Figure 5.3: Time diagram showing the instantaneous link bandwidth over 1-ms intervals (dots), its time moving average (dark gray line), the instantaneous link bandwidth over 100-ms intervals (light gray line) and the sum of the average rate of all active flows (black line). The trace was taken from an OC-12 link on January 18th, 2003 [131].

User flows also provide an advance notice before major changes in bandwidth utilization occur. For example, we can see that in Figure 5.3 there is a sudden increase in traffic between times 21 s and 46 s (due to a single user flow whose only constraint was a 10-Mbit/s link). This traffic increase was predicted four seconds before it happened by observing the active flows. There are two reasons for this advance notice: first, an application may take some time to start sending data at full rate after it connected with its peer.[2] Second, it takes several round-trip times for TCP connections to ramp up their rate to the available throughput because of the slow-start mechanism. In contrast, when we monitor the instantaneous arrival

[2]This is the main reason for the advance notice in Figure 5.3. Unfortunately, it was impossible to know what application caused this behavior because the trace was "sanitized".

rate to estimate the traffic matrix, the filters that are applied to reduce the noise add some delay to the decision making of whether more capacity is needed. If the circuit creation mechanism already takes a long time, adding more delay in the traffic estimation makes the system react more slowly.

5.3 Monitoring user flows

In this chapter, I propose monitoring user flows to estimate the traffic matrix between boundary routers because they can provide a stable (i.e., with little variation) and predictive estimate of the actual traffic. The arrival process of these user flows has in general fewer long- and short-range dependencies. It has been reported that arrivals of user flows in the core behave as if they followed a Poisson process [78]. Feldmann reported that the interarrival times of HTTP flows follow a Weibull distribution [73], but as the link rate increases and more flows are multiplexed together, the interarrival times tend to the special case of the exponential distribution according to Cao et al. [33] and also Cleveland et al. [45]. The Poisson arrival process is well understood and there are many models in queueing theory that use it.

The approach I am proposing requires similar hardware support for monitoring active flows to what was described in Section 4.3, basically a fixed-length classifier that can detect new flows and that monitors the activity of the current flows. Such classifiers are already available for OC-192c link speeds [4, 71]. However, counting the number of active flows is not enough, as we need to know the average bandwidth that they use. Most of the time it is not possible to estimate the average bandwidth when the flow starts because it requires knowing the flow duration and the number of bits that will be transmitted. In contrast, it is possible to have an upper bound, which I will call peak bandwidth[3] of a flow. I consider this flow peak bandwidth to be constant throughout the lifetime of the flow, and it can be determined the same way as in Section 4.3.3 (through signaling or through an estimation of the access link bandwidth) even if one does not know *a priori* the flow average bandwidth.

[3]The only requirement for the flow peak bandwidth is that it has to be larger than the flow average bandwidth.

More formally, once we know the set of active flows between a pair of boundary routers at a given instant, $F(t)$, we need only to assign a peak bandwidth to each of the flows, C_f, where $C_f \geq average\,BW(f), \forall f \in F(t)$. Then, we need a circuit with a capacity, $K_{cct}(t)$, that is greater than or equal to the sum of the flow peak bandwidths, $C(t) = \sum_{f \in F(t)} C_f$ and $K_{cct}(t) \geq C(t)$.

Many circuits take time to be created because circuit management signaling, switch scheduling, and/or crossconnect reconfiguration may be slow. If we decide that we need to increase the circuit capacity between two boundary routers, $C(t)$, there will be some latency, T, before the changes take place. During this latency period, the circuit capacity will be insufficient, and queueing delays and potentially packet drops will occur at the circuit head. I call this a *circuit overflow.* More precisely, a circuit overflow happens at time t when:

$$\{\exists \tau \in [t, t+T), s.t.\ C(\tau) > C(t)\}$$

Obviously, the longer the circuit-creation latency, T, is, the more circuit overflows occur.

A way of avoiding circuit overflows is to provision extra capacity as safeguard. The size of this safeguard band depends on T and the dynamics of traffic, and it determines the probability of a circuit overflow.

I have used several user-flow traces from the Sprint Backbone [170] to analyze the sizes of the safeguard bands based on the signaling delays and the overflow probabilities. Figure 5.4 displays a sample path showing how the safeguard band varies with time for a circuit-creation latency of $T = 1\,\mathrm{s}$. Based on the sum of average bandwidths of the active flows (dashed line) and the sum of the corresponding peak bandwidths,[4] one can construct the instantaneous peak-bandwidth envelope, $C(t)$, depicted as a solid line. The dotted line shows the safeguard-band envelope, i.e., the maximum of the peak-bandwidth envelope in the next T period (= 1 s), $\hat{C}_T(t) = max\{C(\tau); \tau \in [t, t+T)\}$.

[4]In the analysis, the peak flow rate is defined as the minimum number of 56-Kbit/s circuits that are needed to carry the average flow rate. Over 97.5% of the flows fitted within a single 56-Kbit/s circuit. A tighter bound could have been used, as well.

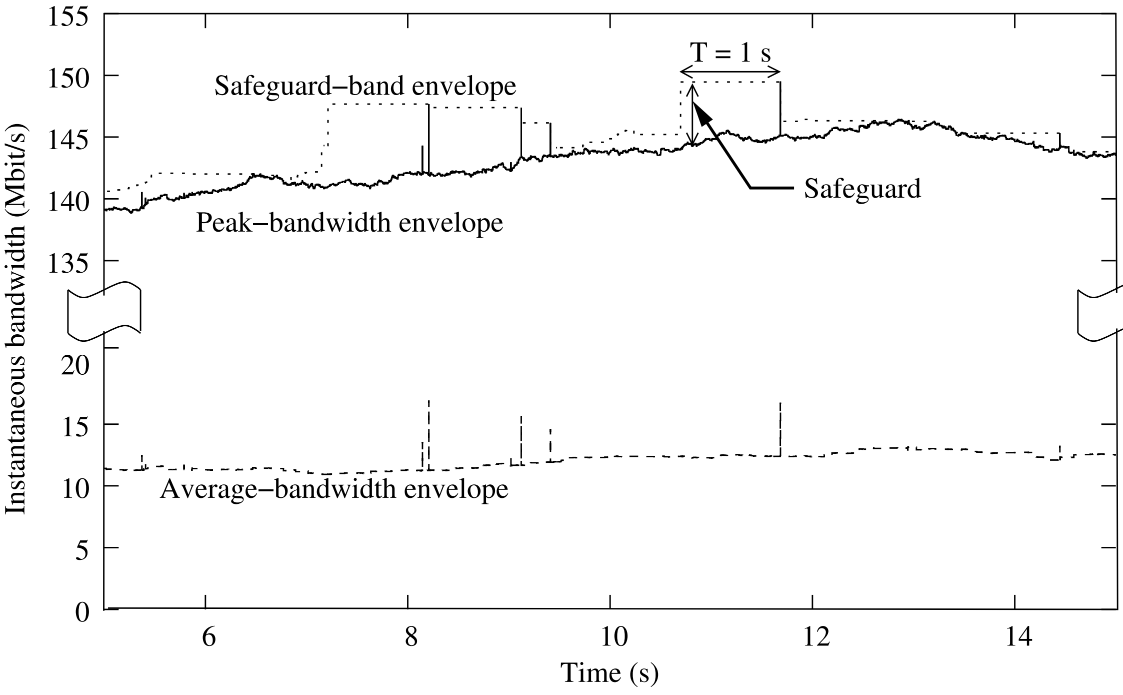

Figure 5.4: Time diagram showing how the safeguard-band envelope is calculated.

Since we cannot predict the future, we can instead analyze $\hat{C}_T(t)$ to find the safeguard band, S_T^p, for a given overflow probability p. In other words, we calculate S_T^p such that $P(\hat{C}_T(t) - C(t) \leq S_T^p \cdot C(t)) \leq p$. In a real system, we would continuously estimate the instantaneous peak-bandwidth envelope, $C(t)$. If at any time the difference between the circuit capacity and $C(t)$ goes below the safeguard band, $K_{cct}(t) - C(t) < S_T^p \cdot C(t)$, then we would request an increase in the circuit capacity, so that the spare capacity remains above the safeguard band to avoid circuit overflows.

Figure 5.5 depicts the safeguard band relative to the peak-bandwidth envelope, $(\hat{C}_T(t) - C(t))/C(t)$, for various overflow probabilities and circuit-creation latencies for one OC-12 link in the Sprint backbone. There are some stair-case steps for a relative safeguard band between 0.04% and 0.3% because the peak-bandwidth envelope can only increase in multiples of 56 Kbit/s, which is around 0.04% of the peak-bandwidth envelope.

Figure 5.5 confirms our intuition that the longer the circuit-creation latency, the larger the safeguard band needs to be for a given overflow probability. For example,

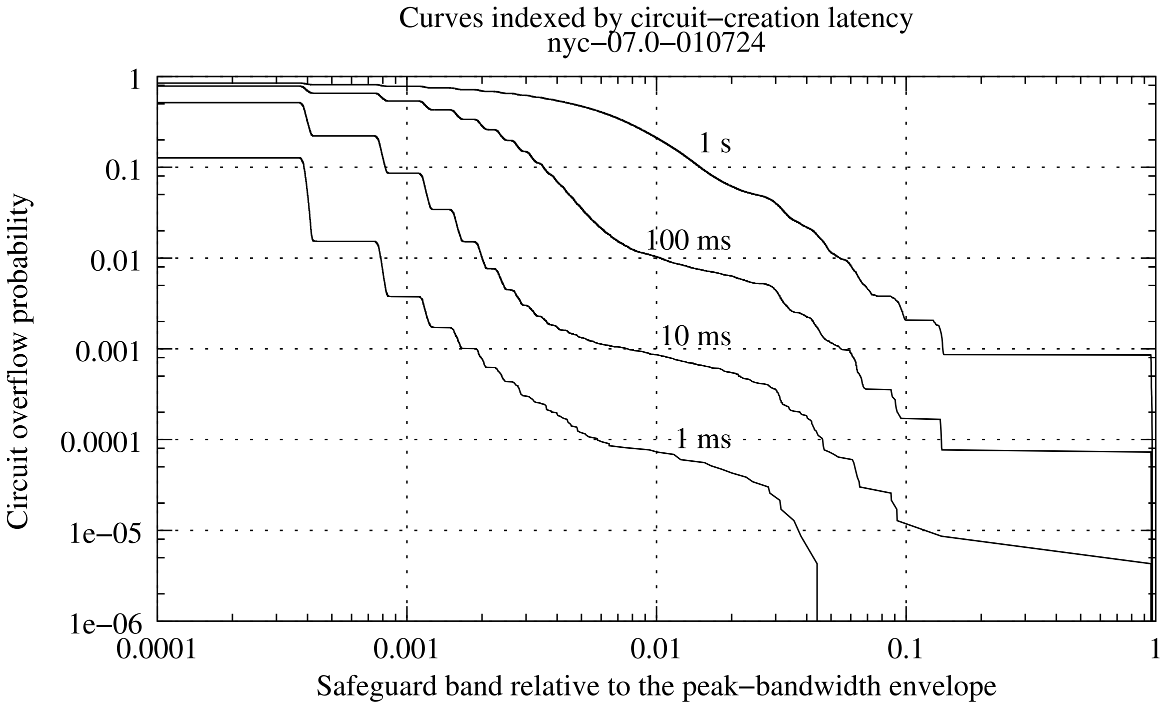

Figure 5.5: Safeguard band required for certain overflow probabilities and circuit-creation latencies.

for an overflow probability of 0.1%, one needs a safeguard of 0.15% times the current peak-bandwidth envelope for T=1 ms, 0.8% for T= 10 ms, 6% for T= 100 ms and 12% for T= 1 s. The faster the crossconnect and the signaling are, the more efficiently resources are used. This result indicates that we should use fast signaling and fast switching elements for the establishment of circuits.

It should also be noted that for safeguard bands greater than or equal to 0.1% of the peak-bandwidth envelope and latencies smaller than or equal to 100 ms, a ten-fold decrease of the circuit-creation latency corresponds to a ten-fold decrease in the overflow probability for the same safeguard band. These results were consistent among all traces that were studied. Figure 5.6 shows the cumulative histogram of the peak-bandwidth envelope for the different Sprint traces. The trace used for Figure 5.5 is the one centered around 150 Mbit/s (nyc-07.0-010724). The other traces yielded similar safety margins.

The liberation of resources is not as important as their reservation because their

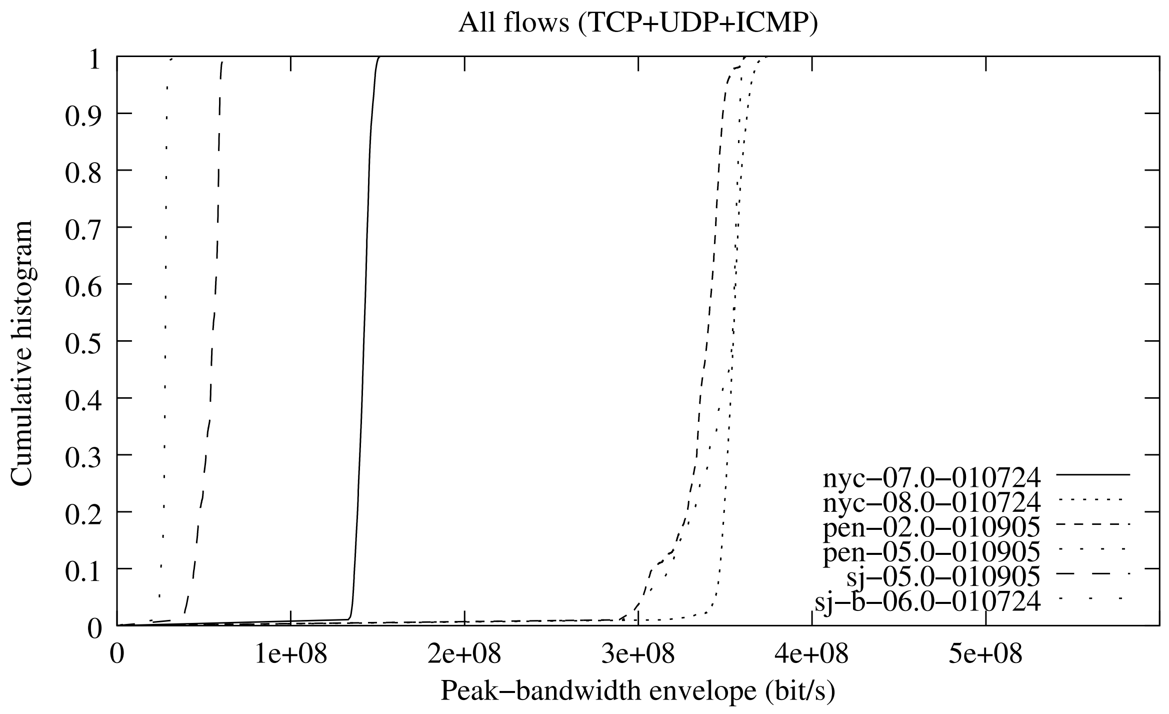

Figure 5.6: Cumulative histogram of the peak-bandwidth envelope for different Sprint traces.

release does not directly contribute to a circuit overflow (unless bandwidth is scarce, but as mentioned in Chapter 2, bandwidth is plentiful in the core). One can simplify the circuit management signaling with a scheme that uses soft state and an inactivity timeout. This simple scheme would retain the extra circuit bandwidth for a period of time that is at least as long as the circuit-creation latency to avoid oscillations in the resource allocation.

5.4 Modeling traffic to help identify the safeguard band

In the previous section, I used traces from real links in the network to predict the safeguard band that is required for a certain overflow probability. In most cases, it is not economical to have trace collecting equipment on every link, and so it may not be possible to obtain such detailed traces. For this reason, it is beneficial to have a simple model that requires less information to achieve the same goal. In addition, if the model is simple enough, one can also obtain formulae that predict the appropriate safeguard band based on a small number of network parameters.

I will now perform the same analysis as in the previous section on synthetic traffic traces that are generated using the distributions and statistics from the links under consideration. Notice that this stochastic information can be obtained with considerably less effort than a real trace because they can be estimated by sampling the traffic.

In a trace of active flows, one has three pieces of information per flow: the flow interarrival time, the flow duration and the flow average bandwidth.[5] Flow interarrival times are essentially independent of each other and closely follow a Poisson process, as shown by the nearly exponential interarrival times in Figure 5.7. In the traces, the average arrival rates were between 124 and 594 flow/s. This hypothesis of Poisson-like arrivals is further supported by the wavelet estimator described by Abry and Veitch [1]: the Hurst parameter of the interarrival times is very close to 1/2, which suggests independence. Similar results have been reported by Fredj et al. [78] and by Cleveland et al. [33, 45]. For this reason, for the synthetic trace, we can model flow arrivals as a Poisson process. Hence to parameterize the model we need only the average arrival rate of the flows.

The flow average bandwidth (shown in Figure 5.8a) and the flow duration (shown in Figure 5.8b) have empirical distributions that are harder to model. Furthermore, the values are not independent of each other. The correlation coefficient between them in the Sprint traces was between -0.134 and -0.299,[6] which is consistent with the work by Zhang et al. [189]. Figure 5.9 shows the joint histogram for the flow duration and average bandwidth, which makes their correlation clear. Jobs with more available bandwidth usually take less time to complete. In terms of successive arrivals, the autocorrelation function was almost zero, and so the arrivals can be considered

[5]One could use the number of bytes transferred by the flow instead of the flow average bandwidth, since the latter is equal to the former divided by the flow duration.

[6]For TCP traffic, the correlation coefficient was between -0.137 and -0.310, whereas for non-TCP traffic, it was between -0.089 and -0.391.

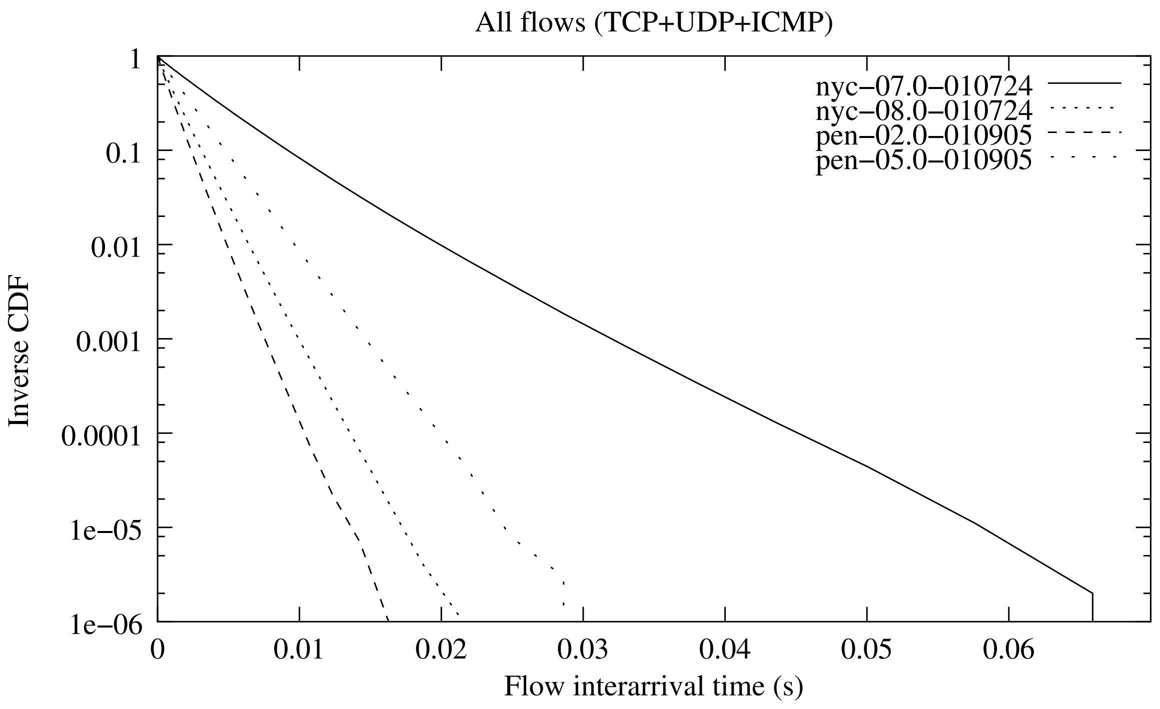

Figure 5.7: Inverse cumulative histogram of the flow interarrivals for both TCP and non-TCP traffic in the Sprint traces. An exponential interarrival time would be represented as a straight line in this graph.

independent. The flow average bandwidth and flow duration can then be modeled as a sequence of i.i.d. 2-dimensional random variables.

Even if the correlation between the flow average bandwidth and the flow duration is small, when the marginal distributions of the two magnitudes are used the results of the model and the traces diverge considerably for the low overflow probabilities. The reason is that short-duration and high-bandwidth flows occur more often in the synthetic traces created from the marginal distributions than in the real trace, and these flows can skew the results. Results are much closer to the trace-driven model when using Poisson arrivals and the empirical joint distribution for the flow duration and average rate. Figure 5.10 shows how the synthetic trace using the joint distribution produces results that are very close to those obtained with the real trace.

This model corresponds to an $MB/G/\infty$ system, where there are infinite parallel servers, arrivals are batched Poisson and service times are correlated with the

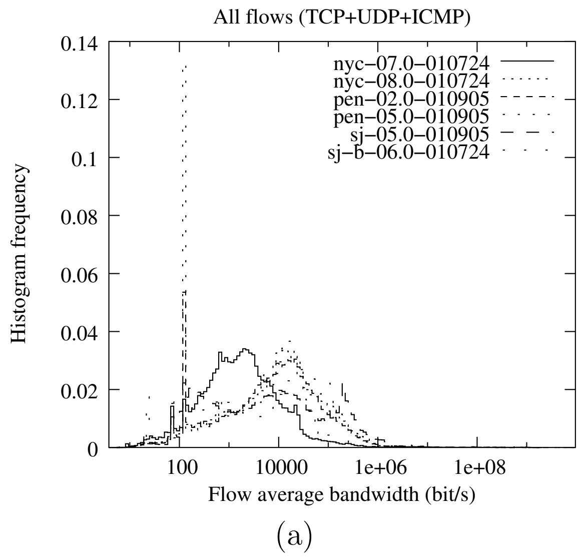

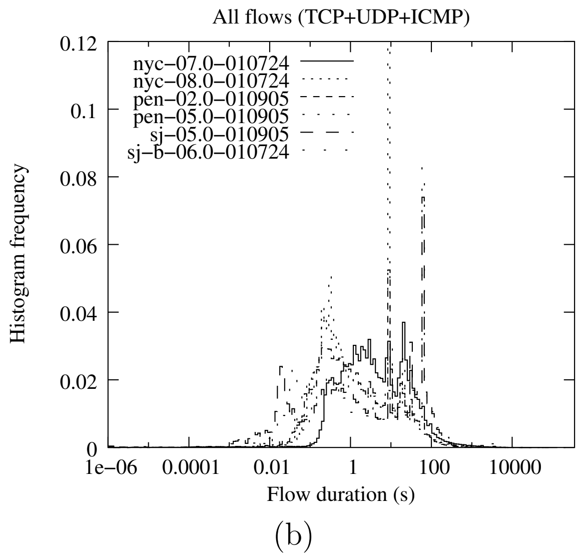

Figure 5.8: Histograms of (a) the flow average bandwidth and (b) the flow duration for both TCP and non-TCP traffic in the Sprint traces. Single-packet flows have not been considered.

batch size. As far as I know, there is no closed-form expression for the transition probabilities:

$$\begin{aligned} p &= 1 - P[N(t) - N(0) < S_T^p \cdot N(0), \forall t \in [0,T)] \\ &= P[max\{N(t) - N(0), \forall t \in [0,T)\} \geq S_T^p \cdot N(0)] \end{aligned}$$

where $N(t)$ is the number of clients in the system at time t.

In summary, we can estimate the safeguard band that is required to avoid circuit overflows just by using the average flow rate and the joint distribution of the flow average bandwidth and the flow duration. This information can then be used to construct a set of curves like the one in Figure 5.10.

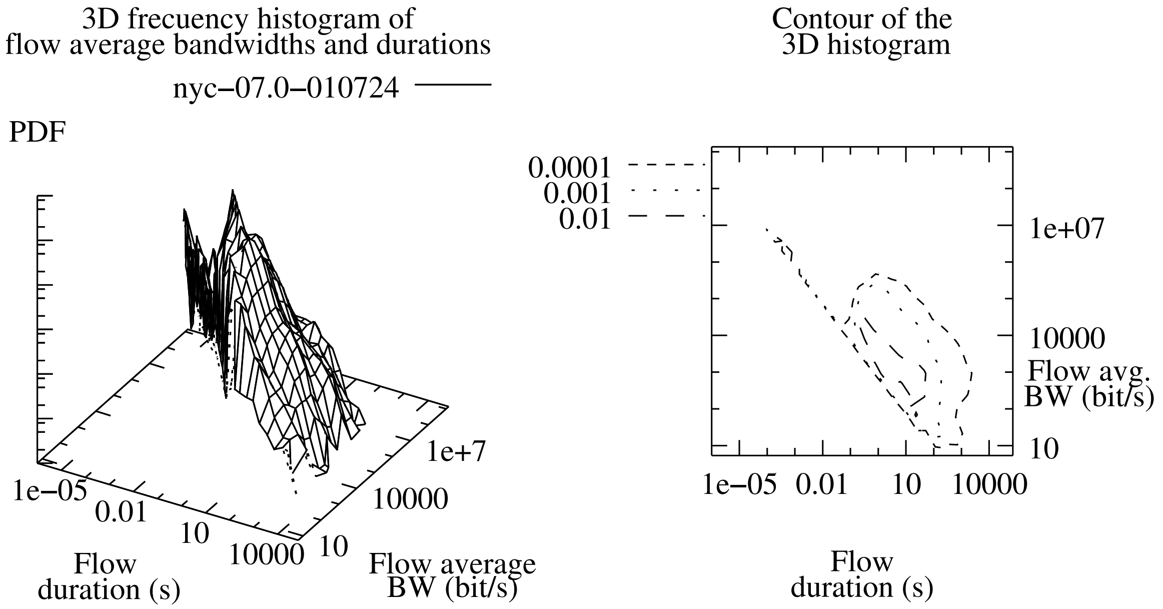

Figure 5.9: Joint histogram of flow durations and average bandwidths for both TCP and non-TCP traffic in the Sprint traces.

5.5 Discussion

This chapter considers circuits between boundary routers. If we need to increase the capacity of an existing circuit, it might be that the current circuit path cannot accommodate this increase, while an alternate path can. In this case, one option is to reroute the whole circuit through a path that has the required capacity (if there is one), but this option might be too costly in terms of signaling and resource consumption. One alternative is to create a separate circuit with a capacity equal to the additional capacity that is needed. However, one problem is that this parallel circuit will have a propagation latency that is different from the original path. If data is injected into the combined circuit, it may happen that a packet is split into two parts that travel through different paths, and so a complex realignment buffer will be required at the egress point to realign the two parts of the packet. Such a mechanism has already been proposed for SONET/SDH, and it is known as virtual concatenation of channels [46, 166].

One way of eliminating this realignment is to avoid splitting packets over parallel

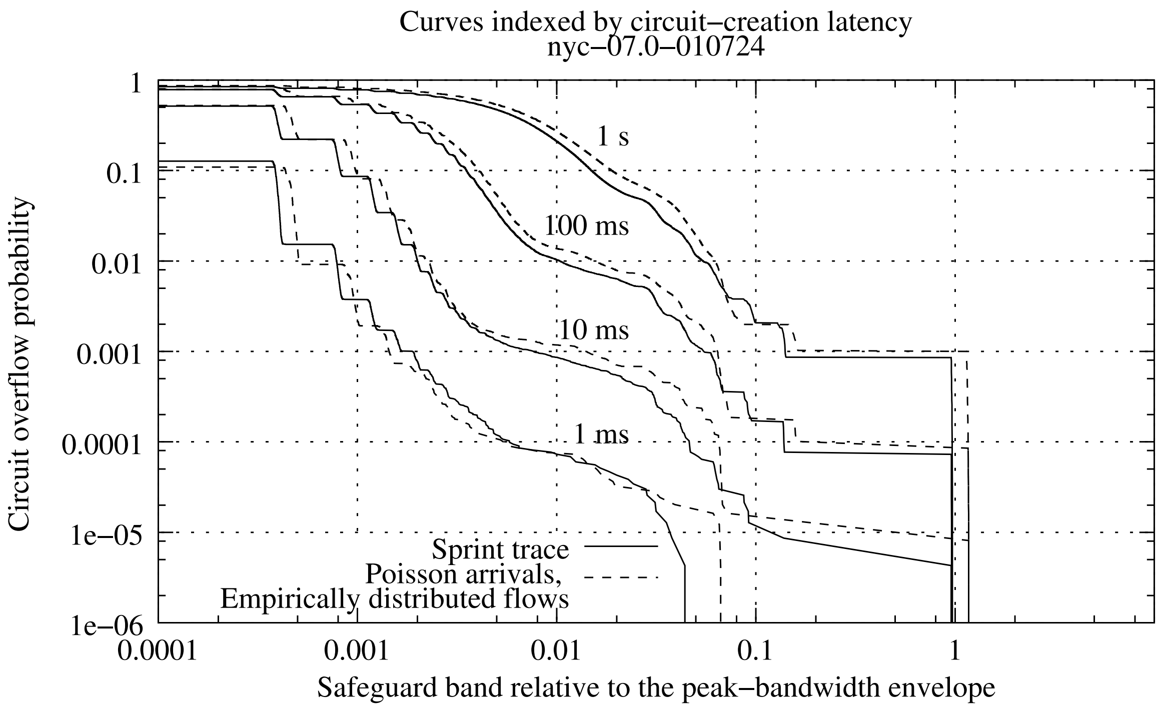

Figure 5.10: Safeguard band required for certain overflow probabilities and circuit-creation latencies for real traffic traces (solid line) and a simple traffic model (dashed line) with Poisson arrivals and flow characteristics that are drawn from an empirical distribution.

paths. Packets can then be recovered integrally at the tail end of each backbone circuit and injected directly into the packet-switched part of the network. This method can create some packet reordering within a user flow, which TCP may interpret as packet drops due to congestion. Yet, reordering would be rare if the difference in propagation delays between the parallel paths is smaller than the interarrival time imposed by the access link to consecutive packets of the same flow (for 1500-byte packets, it is 214 ms for 56-Kbit/s access links, and 8 ms for 1.5-Mbit/s access links). One possible solution is to equalize the delay using a fixed-size buffer at the end of one of the sub-circuits. However, this buffer may not be necessary because, as reported recently [17], TCP is not significantly affected by occasional packet reordering in a network.

It should be pointed out that the definition used here for circuit overflow is rather strict, and it represents an upper bound on the packet drop rate. In general, the ingress boundary router will have buffers at the head end of each backbone circuit, which will absorb short fluctuations in the flow rate between boundary routers. For this reason, in the measurements in Figures 5.5 and 5.10, all single-packet flows were ignored. The buffer at the head end will also allow the system to achieve some statistical multiplexing between active flows; something that TCP Switching in Chapter 4 could not achieve. However, as mentioned in Chapter 3, this statistical multiplexing will not necessarily lead to a smaller response time because the flow peak rate will still be capped by the access link.

The approach presented in this chapter does not specify any signaling mechanism and does not impose any requirements on it. One could use existing mechanisms such as the ones envisioned by GMPLS [7] or OIF [13], which will be described in Chapter 6. This method can also be used in conjunction with TCP Switching to control an optical backbone with an electronic outer core and an optical inner core. TCP Switching would control the outer fine-grain electronic circuit switches and would provide the information that is used to control the inner coarse-grain optical circuit switches.

5.6 Conclusions and summary of contributions

This Chapter has discussed how to monitor user flows to predict when more bandwidth is needed between boundary routers of a circuit-switched cloud in the Internet. It has also developed a simple model that can be used to estimate safeguard bands that compensate for slow circuit-creation mechanisms.

The most important recommendation of this chapter is that the signaling used to establish a circuit should be as fast as possible. Otherwise, the safeguard band becomes very large. An alternative reading of this recommendation is that the establishment of a circuit should be done simultaneously on all nodes along the path, without having to wait for any confirmation from the upstream or downstream nodes. Moreover, slow crossconnect technologies (such as MEMS mirrors) should only be used if they can provide a very large switching capacity at a low cost, such that it can accommodate the additional safeguard band.